RSC Advances

PAPER

View Article Online
View Journal | View Issue

Cite this: *RSC Adv.*, 2025, **15**, 40299

Gamma radiation-induced molecular transformation of hydrocarbons in the presence of nanostructured sodium bentonite clay

M. K. Ismayilova, *[a] I. I. Mustafayev, [ab] R. F. Khankishiyeva, [abd] H. N. Akhundzada, [acde] S. Z. Melikova [a] and R. A. Bayov [a]

Received 21st July 2025
Accepted 14th October 2025

DOI: 10.1039/d5ra05244k

rsc.li/rsc-advances

This study investigates the molecular transformation of hydrocarbons under gamma radiation in the presence of nanostructured sodium bentonite clay. Crude oil samples from the Gunashli oil field (Azerbaijan) were exposed to ^{60}Co gamma radiation across a dose range of 0–260 kGy. Using a combination of FTIR, UV-vis, EPR spectroscopy, and gas chromatography, we evaluated the structural evolution of both mature and immature oils. The results demonstrate a dose-dependent degradation of aromatic compounds, accompanied by increased formation of isomeric and low-molecular-weight hydrocarbon gases. Nanostructured Na-bentonite acted as a radiation-sensitive catalyst, significantly enhancing fragmentation, isomerization, and π–σ bond transformation. In mature oils, a pronounced reduction in arenes and density confirmed advanced molecular restructuring. In contrast, immature oils retained substantial aromatic content, indicating partial metamorphism. UV-vis data revealed a sequential transformation pathway from polycyclic aromatics to saturated hydrocarbons. The findings underscore the catalytic synergy between gamma radiation and nanoclay, offering mechanistic insights into radiolytic upgrading and mimicking natural geochemical maturation processes.

1 Introduction

The thermal interaction of organic compounds—particularly hydrocarbons—with clay minerals has long attracted scientific attention due to its significance in petroleum geochemistry and catalysis. Numerous studies have demonstrated that the active sites of clay minerals, especially those located within their interlayer spaces, significantly accelerate the thermal degradation of organic matter.[1–9] These minerals are widely recognized as key catalysts in the transformation of organic material into petroleum and natural gas. A widely accepted hypothesis posits that light hydrocarbons act as intermediates during the catalytic conversion of petroleum into gas, following the pathway: petroleum → light hydrocarbons → gas.[10]

Growing evidence supports the view that clay minerals play a central role in determining the molecular architecture of hydrocarbons throughout these transformation processes. Among these, montmorillonite—particularly in the presence of bitumen—exhibits enhanced catalytic activity for generating light hydrocarbons when compared to other organic sources such as kerogen or asphaltenes. This effect is likely attributable to the smaller molecular size of bitumen, which facilitates its interaction with the active catalytic sites on the clay surface.[11]

In recent years, the interaction between ionizing radiation and clay-hydrocarbon systems has gained attention, particularly for its potential to induce chemical and physicochemical changes. In this study, gamma radiation from cobalt-60 (^{60}Co) was employed to investigate such effects on nanostructured sodium bentonite clay, sourced from the Republic of Azerbaijan. The clay samples were subjected to gamma radiation doses ranging from 1 to 260 kGy under vacuum conditions. Subsequent analyses using thermogravimetric analysis (TGA) and Fourier-transform infrared spectroscopy (FTIR) revealed that nanostructured Na-bentonite displays increased chemical reactivity under these conditions.[12]

The structural transformation of hydrocarbons—commonly referred to as metamorphism—occurs predominantly at the molecular level. Previous research indicates that gamma radiation induces dehydration reactions on the surface of Na-bentonite, generating structural defects that can significantly affect hydrocarbon chain behavior. These effects include chain scission, radical formation, and subsequent recombination, which ultimately influence the molecular weight and configuration of the hydrocarbons.[13–17]

[a]*Institute of Radiation Problems, Ministry of Science and Education of the Republic of Azerbaijan, Baku AZ1143, Azerbaijan*
[b]*Azerbaijan University of Architecture and Construction, Baku AZ1073, Azerbaijan*
[c]*Scientific-Research Institute «Geotechnological Problems of Oil, Gas and Chemistry», Azerbaijan State Oil and Industry University, Baku AZ1010, Azerbaijan*
[d]*Research Institute of Crop Husbandry, Ministry of Agriculture of Azerbaijan Republic, Baku, AZ1135, Azerbaijan*
[e]*ICESCO Biomedical Materials Department, Baku State University, Z. Khalilov Str. 23, Baku, AZ1148, Azerbaijan. E-mail: ismayilovamehpara@gmail.com*

Furthermore, the mechanisms underlying the formation of aromatic hydrocarbons and isomeric structures under gamma irradiation have been examined in various studies.[18,19] Comparative investigations show that in aromatics-rich crude oils—such as those from the Gunashli oil field in Azerbaijan—low-dose gamma irradiation in the presence of nanostructured catalysts promotes the formation of isomeric structures. In contrast, crude oils with low aromatic content are more prone to form new aromatic compounds under similar conditions.

This study aims to investigate the role of gamma irradiation in the molecular transformation of hydrocarbons in crude oil and to evaluate the effectiveness of nanostructured sodium-bentonite clay as a radiation-sensitive catalyst simulating natural maturation processes.

2 Materials and methods

2.1 Sample collection and characterization

Crude oil samples were collected from three distinct production platforms (platforms 8, 10, and 14) located in the Gunashli oil field (Azerbaijan sector of the Caspian Sea). Samples from platforms 8 and 10 were obtained from mature wells, whereas the sample from platform 14 originated from a relatively immature reservoir.

2.2 Sample preparation and irradiation

Nanostructured sodium bentonite clay, with an average particle size of 40–70 nm, was sourced locally from the Republic of Azerbaijan. For each experimental run, 0.20 g of Na-bentonite was accurately weighed into 15 mL quartz ampoules. Subsequently, 1.00 mL of the crude oil sample was added, maintaining a fixed clay-to-oil mass ratio of 1 : 5. This ratio was selected to ensure consistent and reproducible interaction between the clay catalyst and the oil matrix across all experiments. The ampoules were degassed under vacuum, and cryogenically frozen in liquid nitrogen. Following freezing, a controlled amount of oxygen was introduced into the system to induce partial oxidation of the bentonite surface. The ampoules were then hermetically sealed under static vacuum conditions. Gamma irradiation was performed at ambient temperature using a sealed ^{60}Co radiation source. The dose rate was maintained at 10.05 rad s^{-1}, and the irradiation time was varied between 0 and 300 hours, corresponding to total absorbed doses ranging from 0 to 260 kGy. The detailed procedure is presented in Fig. 1.

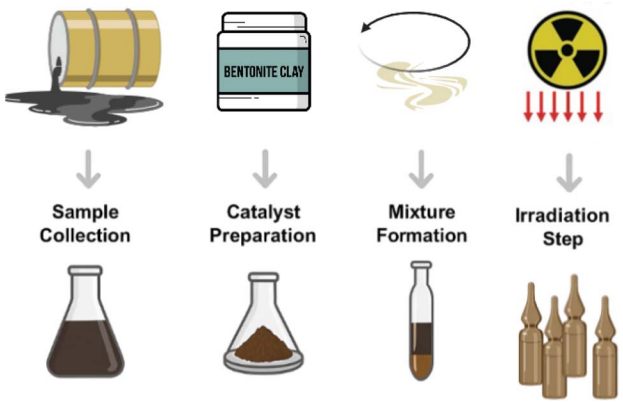

Fig. 1 Experimental workflow for gamma-irradiated crude oil with Na-bentonite clay.

2.3 Analytical techniques

2.3.1 Density and rheological properties. Kinematic viscosity was measured using a Hess-type capillary viscometer. The dynamic viscosity was calculated by multiplying the kinematic viscosity by the corresponding density value, in accordance with ASTM D445-19 $\times$ 10^1 standard.

2.3.2 Gas chromatography (GC). Radiolytic gaseous products were analyzed using Gazchrom-3101 and Svet-101 gas chromatographs. The analytical system provided a hydrogen detection sensitivity of $K(H_2) = 6.0 \times 10^{13}$ molecules·$(cm^3 mm)^{-1}$, enabling quantification of trace gas components generated during irradiation.

2.3.3. Electron paramagnetic resonance (EPR). EPR measurements were conducted using a Bruker EMX PLUS spectrometer operating in the X-band region (9.75 GHz, $\lambda \approx 3$ cm). The applied magnetic field range was 0–6000 G (0–600 mT). This technique was employed to detect and characterize paramagnetic species, particularly free radicals formed during gamma irradiation of the crude oil-clay systems.

2.3.4 Fourier-transform infrared spectroscopy (FTIR). FTIR measurements were conducted using a Varian 640 spectrometer to evaluate changes in the vibrational spectra of both crude oil samples and nanostructured bentonite clay before and after irradiation.

2.3.5 UV-vis spectroscopy. The optical absorption spectra (ultraviolet and visible range) of the studied samples were measured using a Cary 50 Scan spectrophotometer (Varian) in the wavelength range of $\lambda = 200$–800 nm. Changes in spectral features as a function of gamma irradiation dose were analyzed to elucidate the transformation pathways of aromatic and polycyclic hydrocarbon structures.

2.4 Rheological and compositional data

Table 1 presents the physical properties of the crude oil samples. The immature oil from platform 14 exhibited significantly higher density and viscosity, along with elevated aromatic content, compared to the mature oils from platforms 8 and 10.

Table 1 Physical properties and aromatic content of crude oil samples from the Gunashli oil field (25 °C, 1 atm)

Parameter	Platform 8 (mature)	Platform 10 (mature)	Platform 14 (immature)
Density (g cm^{-3})	0.8553	0.8547	0.9302
Kinematic viscosity (cm^2 s^{-1})	12.6	9.9	61.5
Dynamic viscosity (mPa s)	10.78	8.46	57.21
Aromatic content (wt%)	—	—	25

3 Results and discussion

3.1 FTIR spectral characterization of crude oil samples from the gunashli field

Fourier-transform infrared (FTIR) spectroscopy was employed to elucidate the molecular features of crude oil samples collected from three distinct production platforms (no. 8, 10, and 14) within the Gunashli oil field. The primary objective was to differentiate the aliphatic and aromatic hydrocarbon fractions and assess the maturity of the samples based on functional group distributions. Representative FTIR spectra are presented in Fig. 2.

Fig. 2a displays the FTIR spectrum of the crude oil from platform no. 8, representative of a thermally mature sample. Prominent absorption bands at 2924 cm^{-1} and 2849 cm^{-1} correspond to the asymmetric and symmetric C–H stretching modes of aliphatic $–CH_3$ groups, respectively. A moderate band observed at 1605 cm^{-1} is attributed to C=C stretching vibrations of aromatic systems. The bending modes at 1460 cm^{-1} and 1378 cm^{-1} further support the dominance of long-chain aliphatic hydrocarbons, characteristic of mature oil.

In contrast, the spectrum of the sample from platform no. 14 (Fig. 2b), classified as immature, reveals substantially enhanced absorption at 1605 cm^{-1}, indicative of a higher aromatic content. This is corroborated by the appearance of an intense band at 819 cm^{-1}, corresponding to the out-of-plane bending of aromatic C–H bonds. A broad band in the vicinity of 3160 cm^{-1} suggests the presence of hydroxyl (–OH) functionalities or moisture absorption. These observations align with the physicochemical data (Table 1), which report increased aromatic content (~25 wt%) and elevated viscosity for this sample.

Fig. 2c presents the FTIR spectrum of the platform no. 10 sample, which also reflects mature oil characteristics. While similar in spectral profile to platform no. 8, the slightly elevated intensity at 1605 cm^{-1} suggests a moderate aromatic component. The distinct band near 726 cm^{-1} may be associated with long-chain linear alkanes and their crystalline domains.

A comparative evaluation of the spectra highlights a clear trend between oil maturity and the balance of aliphatic *versus* aromatic functional groups. Immature oils exhibit more intense aromatic features, whereas mature samples are predominantly aliphatic. This observation is consistent with established thermal maturation processes, wherein aromatic structures persist in less evolved oils due to limited thermal degradation.

Overall, FTIR analysis provides valuable insight into the compositional variability of crude oils across the Gunashli field. Diagnostic vibrational bands, including those for –CH, C=C, C=O, and –OH moieties, serve as reliable indicators for assessing oil quality and maturity.

3.2 Dose-dependent formation of hydrocarbon gases in catalyzed and non-catalyzed mature oil systems

The formation of low-molecular-weight hydrocarbon gases during γ-irradiation of mature crude oil was investigated over a dose range of 0–250 kGy. Experiments were conducted both in the absence and presence of nanostructured Na-bentonite clay as a catalytic additive. The concentrations of radiolysis products—including CH_4, C_2H_6, C_2H_4, and grouped hydrocarbon fractions ($\sum C_3$ to $\sum C_8$)—were determined and analyzed as functions of absorbed dose. The results are illustrated in Fig. 3a–i, where Ni denotes the concentration of each gas in units of 10^{-16} molecules mL^{-1} and D is the irradiation dose in kGy.

3.2.1 Methane (CH_4). As the dominant product, methane showed a sharp increase in concentration up to ~100 kGy, followed by a plateau at higher doses (Fig. 3a). The catalytic system

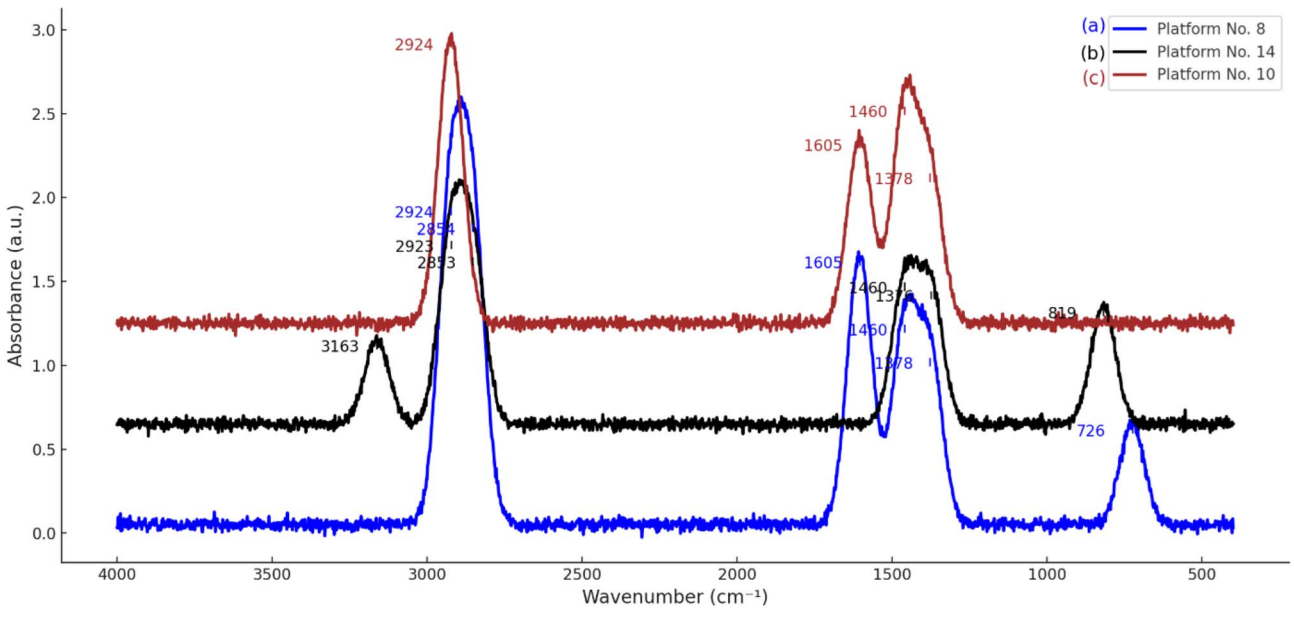

Fig. 2 FTIR spectra of crude oil samples obtained from the Gunashli oil field: (a) platform no. 8 (mature oil); (b) latform no. 14 (immature oil); (c) latform no. 10 (mature oil).

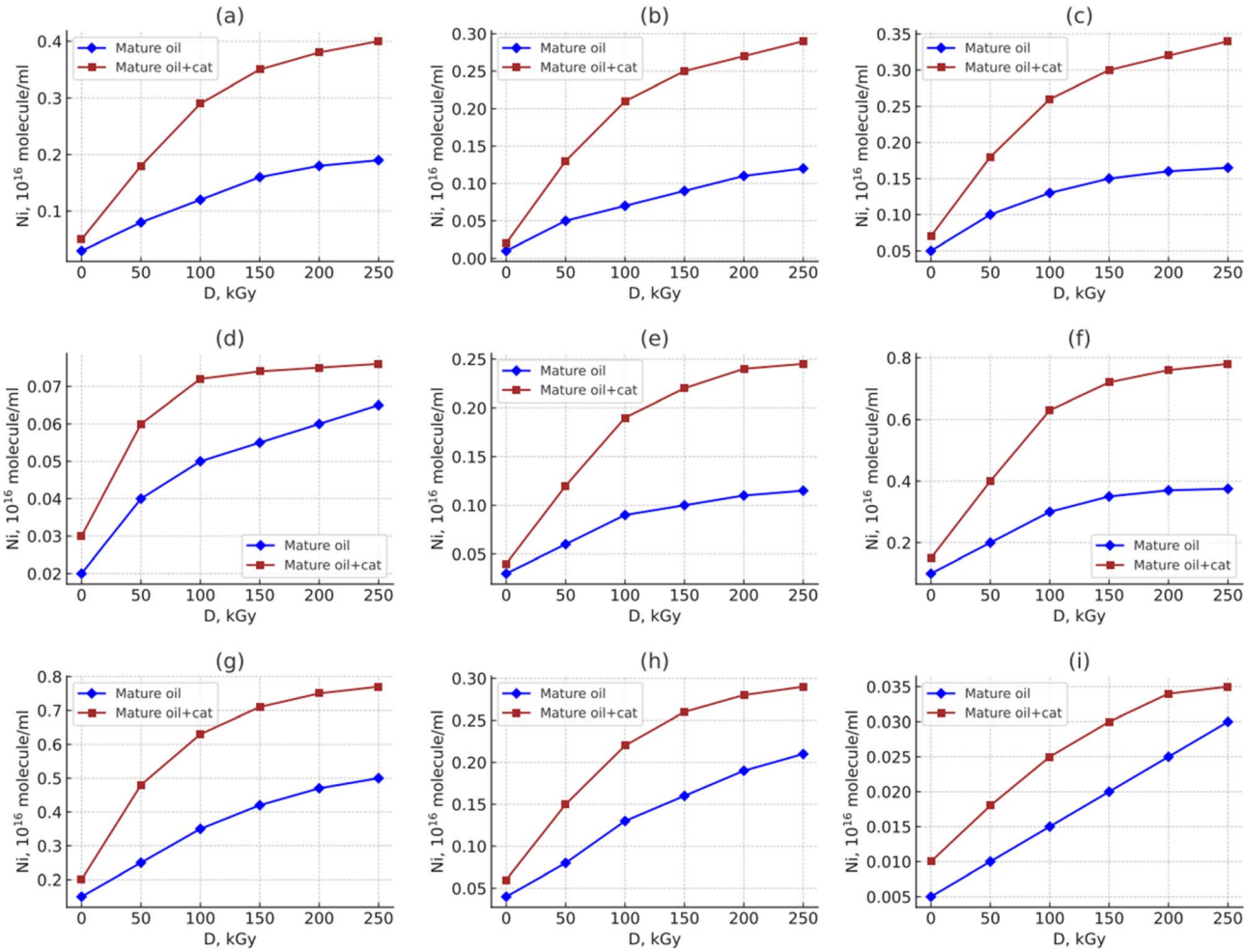

Fig. 3 Effect of irradiation dose (D, kGy) on the concentration (Ni, 10^{-16} molecules mL^{-1}) of hydrocarbon gases formed during γ-radiolysis of mature crude oil samples, with and without Na-bentonite catalyst: (a) CH_4, (b) C_2H_6, (c) C_2H_4, (d) $\sum C_3$, (e) $\sum C_4$, (f) $\sum C_5$, (g) $\sum C_6$, (h) $\sum C_7$, (i) $\sum C_8$.

nearly doubled the CH_4 yield compared to the non-catalyzed sample, particularly above 150 kGy, suggesting enhanced C–C bond cleavage in the presence of Na-bentonite.

3.2.2 Ethane, ethylene, and C_3 hydrocarbons. Fig. 3b–d present the dose-response curves for C_2H_6, C_2H_4, and $\sum C_3$. The formation of these gases also followed nonlinear trends, with saturation occurring at higher doses. Catalytic conditions significantly increased the formation of ethane and $\sum C_3$, while ethylene exhibited a more moderate increase—likely due to its higher reactivity and possible consumption in secondary reactions.

3.2.3 C_4 to C_6 hydrocarbons. Production of C_4, C_5, and C_6 hydrocarbons (Fig. 3e–g) increased substantially in catalyzed systems. The yields were 2–3 times higher than those of non-catalyzed samples. A plateau observed beyond ~100 kGy suggests a transition from primary bond scission to secondary recombination or rearrangement processes.

3.2.4 C_7 and C_8 hydrocarbons. Fig. 3h and i show the formation of heavier volatile hydrocarbons ($\sum C_7$ and $\sum C_8$), which, although present in smaller quantities, also demonstrated a dose-dependent increase and marked catalytic enhancement. These species likely form through recombination or oligomerization of smaller fragments, processes that are facilitated on the surface of the nanostructured clay.

3.2.5 Catalytic impact and mechanistic insight. Across all hydrocarbon groups, the presence of the nanostructured catalyst led to consistently higher gas yields, especially at low to intermediate doses (≤100 kGy). This suggests that Na-bentonite not only promotes early-stage radiolytic cleavage but may also stabilize reactive intermediates, preventing their recombination into less volatile species. At higher doses, a saturation effect indicates the exhaustion of easily cleavable molecular structures within the oil matrix.

3.3 Platform-specific gas evolution behavior in the presence and absence of Na-bentonite catalyst

To evaluate how oil composition and platform-specific characteristics influence radiolytic gas formation, crude oil samples from platform 8 and platform 10 were irradiated under both catalytic and non-catalytic conditions. The dose-dependent

yields of hydrogen and hydrocarbon gases (CH_4 to $\sum C_8$) are shown in Fig. 4a–j.

3.3.1 Hydrogen and light hydrocarbons (H_2, CH_4, C_2H_6, C_2H_4). Platform 10, especially under catalytic conditions, produced significantly more H_2 (Fig. 4a) and CH_4 (Fig. 4b) compared to platform 8. The Na-bentonite catalyst enhanced the formation of ethane (Fig. 4c) in both oils, while ethylene (Fig. 3d) was generated in greater amounts in non-catalyzed

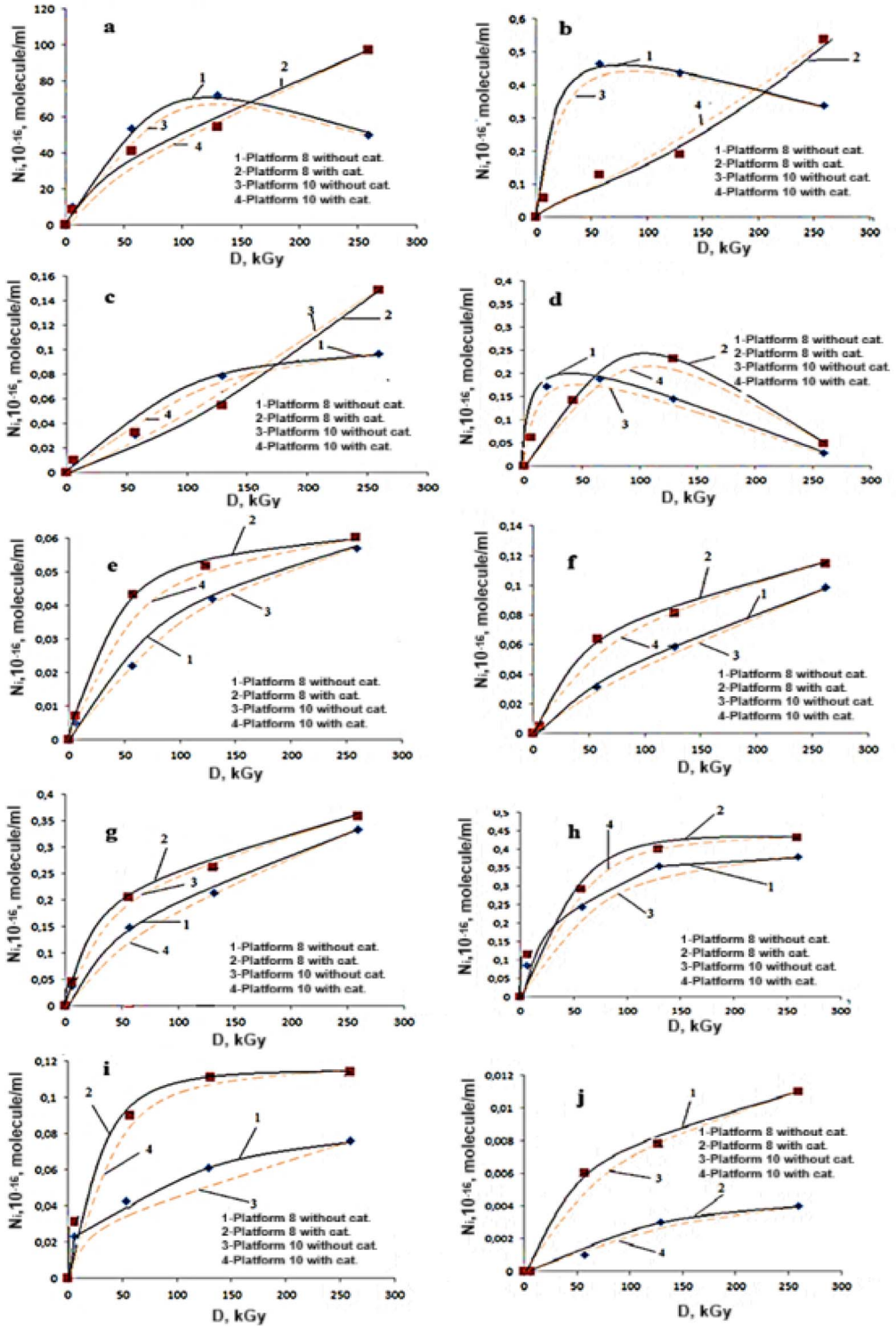

Fig. 4 Dose-dependent formation of molecular hydrogen and hydrocarbon gases (CH_4 to $\sum C_8$) in crude oil samples from platform 8 and platform 10 under gamma irradiation, with and without Na-bentonite catalyst.(a) H_2, (b) CH_4, (c) C_2H_6, (d) C_2H_4, (e) $\sum C_3$, (f) $\sum C_4$, (g) $\sum C_5$, (h) $\sum C_6$, (i) $\sum C_7$, (j) $\sum C_8$.

platform 8 oil, suggesting distinct fragmentation routes depending on platform origin.

3.3.2 C_3–C_6 hydrocarbons. The $\sum C_3$–$\sum C_6$ fractions (Fig. 4e–h) exhibited similar trends, with catalytic systems consistently producing higher gas concentrations. Platform 10 showed a greater response to radiation, likely due to its higher aliphatic and lower aromatic content.

3.3.3 Higher hydrocarbons (C_7 and C_8). The formation of heavier hydrocarbons ($\sum C_7$ and $\sum C_8$; Fig. 3i–j) occurred mostly at higher doses (≥100 kGy), and was more pronounced in catalyzed systems. The near-overlap of catalyzed and non-catalyzed curves in platform 8 suggests molecular rigidity that limits catalytic enhancement.

Overall, Na-bentonite significantly increased gas formation across all systems, but the extent of enhancement depended on the oil's initial composition. platform 10 oils were more responsive, indicating the importance of molecular structure in determining radiolytic reactivity.

Further analysis reveals that at doses below ~50 kGy, the catalytic systems already show significantly higher gas yields, especially in light hydrocarbons. Saturation behavior is observed beyond 150 kGy, indicating depletion of radiation-sensitive moieties. In the case of $\sum C_8$ species, formation was not detected at low doses and appeared only after 57 kGy, consistent with the recombination of smaller fragments at elevated radiation levels.

Additionally, structural transformations in the liquid phase were detected in aromatic-rich oils. Changes in arenes and their isomeric derivatives, particularly in platform 14 samples, confirmed radiation-induced molecular rearrangement. This further emphasizes that the efficiency of radiolytic conversion is not only dose-dependent but also highly sensitive to oil structure.

These findings underscore the synergistic role of gamma radiation and nanostructured catalysts in governing hydrocarbon fragmentation and recombination pathways—critical for advancing radiolysis-based upgrading technologies.

3.4 Structural rearrangement of aromatic compounds under gamma irradiation

To further investigate the effect of gamma irradiation on the molecular structure of crude oil, the concentrations of arenes and their isomeric derivatives in the liquid phase were monitored across a range of irradiation doses (0.7–260 kGy). The experimental data, presented in Fig. 5, reveal a distinct transformation trend influenced by the absorbed dose.

At the lowest dose of 0.7 kGy, arenes dominate the molecular profile, accounting for 25% of the mixture, while isomeric compounds are limited to only 7.5%. As the irradiation dose increases, a progressive decrease in arene concentration is observed, accompanied by a corresponding increase in the concentration of isomeric structures, which reaches 60% at 260 kGy.

This inverse relationship suggests that gamma irradiation induces restructuring of the aromatic core, leading to the formation of positional and structural isomers. The increasing formation of isomers with dose implies the involvement of radiation-induced π-electron delocalization, ring contraction or expansion, and possibly partial saturation or migration of substituents under the influence of energetic radicals.

These results strongly support the hypothesis that gamma radiation facilitates molecular rearrangement, especially in aromatics, and that the presence of a nanostructured catalyst (such as Na-bentonite used in this study) may enhance these processes through surface activation and radical stabilization.

The structural transformation from stable arenes to more reactive isomeric species not only alters the chemical composition of the crude oil but also potentially improves its downstream reactivity and cracking behavior under refining conditions. This metamorphism of the oil matrix under radiation exposure is crucial for understanding radiolytic upgrading mechanisms.

As the radiation dose increases, the content of arenes (1) decreases, while the content of isomeric compounds (2) significantly increases, indicating radiation-induced molecular rearrangement.

3.5 Transformation pathways of polycyclic aromatic hydrocarbons under ionizing radiation: evidence from UV spectroscopy

To further elucidate the structural metamorphism of crude oil samples under ionizing radiation, a schematic transformation pathway of polycyclic aromatic hydrocarbons (PAHs) to alkanes was proposed. This transformation occurs progressively as the radiation dose increases and can be confirmed *via* UV-vis spectroscopy. UV-vis spectra confirmed a dose-dependent transformation of PAHs in mature oils (latforms 8 and 10). With increased gamma dose, absorbance peaks corresponding to anthracene (~375 nm), naphthalene (~275 nm), and benzene (~255 nm) systematically disappeared. The sequential transformation pathway was identified as.

The Scheme 1 illustrates the interconversion of benzene, cyclohexane, cyclopentene, and various branched and linear alkanes, representing typical isomerization and ring-opening reactions involved in hydrocarbon processing.

Hydrocarbon transformation pathways play a crucial role in understanding isomerization, ring-opening, and cracking processes in organic and petrochemical chemistry.

Anthracene (3-ring PAH) → naphthalene (2-ring PAH) → benzene derivatives → cycloalkanes → Alkanes.

This sequential degradation of condensed aromatic systems is characteristic of mature crude oils exposed to gamma radiation. The UV absorption spectra for crude oil samples obtained from platforms 8 and 10—classified as mature oils—are illustrated in Fig. 10a–d. These figures show a gradual loss in the characteristic absorption bands of aromatic compounds as the dose increases.

- Fig. 6a: presence of anthracene, naphthalene, and benzene derivatives.
- Fig. 6b: disappearance of anthracene bands, persistence of naphthalene and benzene derivatives.
- Fig. 6c: only benzene-type signals remain.

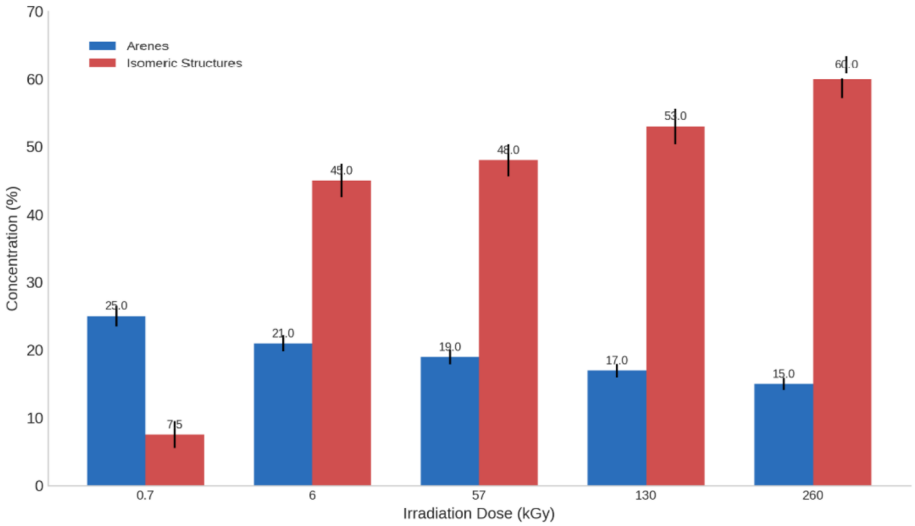

Fig. 5 Correlation between gamma irradiation dose and the concentration of arenes and isomeric structures in aromatic crude oil.

• Fig. 6d: complete disappearance of aromatic absorption, indicating transition to saturated hydrocarbons.

These results demonstrate the radiation-induced transformation of aromatic systems toward aliphatic structures and confirm the completion of metamorphic processes in mature oils. The UV spectral analysis conclusively shows that arenes are nearly depleted at higher doses.

By contrast, the UV spectrum of the immature crude oil sample obtained from platform 14 (Fig. 6) still exhibits prominent aromatic absorption bands even at elevated radiation doses. This suggests that the metamorphic conversion of aromatic hydrocarbons has not yet reached completion in these samples, consistent with their lower maturity level.

3.6 Structural dynamics of arenes in immature crude oil under gamma irradiation (platform 14)

Fig. 7 illustrates the variation in density as a function of gamma irradiation dose for immature crude oil derived from platform 14. This oil sample, characterized by incomplete thermal maturation, provides a valuable model for studying radiation-induced structural transformations of aromatic compounds in crude matrices.

The graph clearly shows that, despite increasing doses of gamma radiation (up to 260 kGy), arenes are not completely decomposed. Instead, their progressive transformation reflects partial degradation, ring-opening, and molecular rearrangements rather than complete elimination. This behavior confirms the relative stability of certain aromatic frameworks and highlights their resistance to radiolytic cracking under moderate irradiation conditions.

In the broader context of metamorphism studies conducted on crude oil from the Guneshli field, this experiment aimed to clarify how gamma dose influences the molecular composition and structure of immature oils. The analysis, based on physicochemical methods, revealed dynamic changes in both aromatic arenes and their isomeric derivatives, confirming the role of radiation in altering the internal structure of the oil matrix.

It is proposed that intermediate radiolytic fragments interact with surface-active environments to form new molecular entities, including hydrides, alkylated species, organosilicon copolymers, and π-complexes containing phenyl, diphenyl, or anthracene-like units. Polycyclic aromatic hydrocarbons (PAHs) with three or more rings (*e.g.*, anthracene, tetracene) are

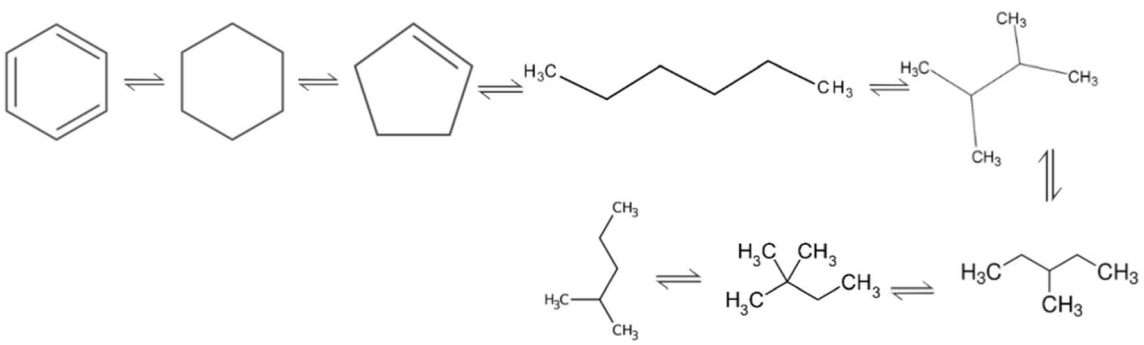

Scheme 1 Structural transformations of hydrocarbons from aromatic to aliphatic forms.

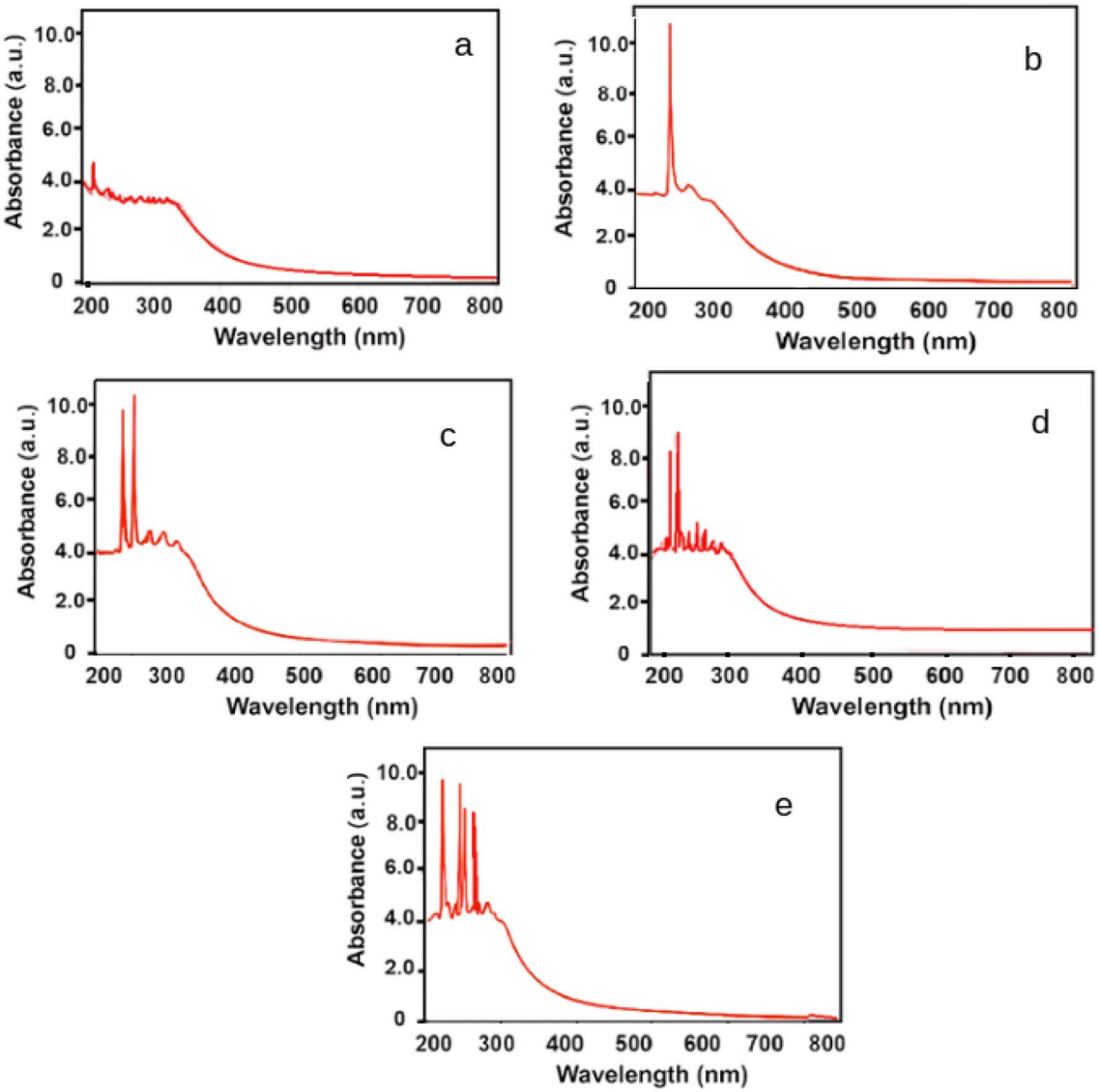

Fig. 6 UV spectra showing the transformation of condensed polycyclic aromatic hydrocarbons in crude oil samples from the Guneshli field under increasing radiation doses. (a) Anthracene + naphthalene + benzene derivatives; (b) naphthalene + benzene derivatives; (c) benzene derivatives only; (d) absence of aromatic bands – full transformation; (e) persistent aromatic peaks in immature crude oil from platform 14.

particularly reactive toward dienes such as butadiene, enabling [4 + 2] cycloaddition (Diels–Alder-type) reactions even at relatively low temperatures. The condensation tendency follows the order: benzene > diphenyl > tetracene > anthracene > naphthalene.

These mechanistic insights suggest that the intermediate fragments generated during irradiation can readily undergo further transformations in the presence of surface-active agents, yielding a range of condensed-phase π-complexes and polymer-like species. The results support the conclusion that radiation-induced metamorphism of immature crude oil leads to a gradual reorganization of its aromatic core, potentially improving reactivity and selectivity for downstream processes such as catalytic cracking or functionalization.

Despite high radiation doses, aromatic compounds are not completely degraded, reflecting their structural stability and partial conversion into isomeric and rearranged derivatives.

3.7 Radiation-induced structural transformation of aromatic hydrocarbons in crude oil

Gamma irradiation of crude oil samples from the Guneshli oil field has revealed significant differences in their structural reactivity depending on oil maturity and initial aromatic content. Experimental findings demonstrated that irradiation of immature oils, particularly from platform 14, promoted the formation of condensed aromatic hydrocarbons such as naphthalene, anthracene, and phenanthrene. These transformations occur through a sequence of radiation-catalytic reactions,

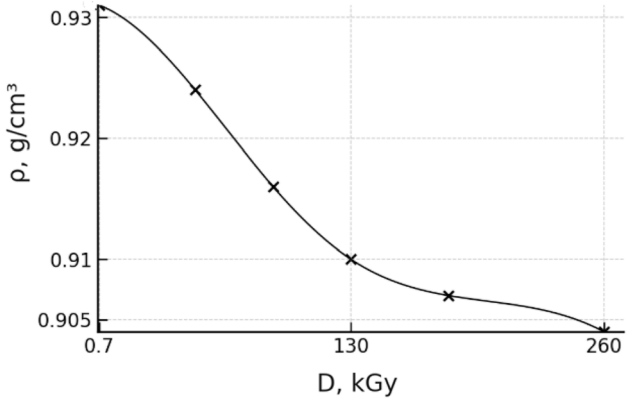

Fig. 7 Variation in density (ρ, g cm^{-3}) of immature crude oil from platform 14 as a function of gamma irradiation dose (D, kGy), indicating progressive transformation of arenes.

driven by reactive intermediates formed during the radiolysis of hydrocarbon chains.

Proposed pathways for aromatic hydrocarbon enrichment include:

$$C_6H_5^+ + C_6H_5^+ \rightarrow C_{10}H_8 + C_2H_2$$

$$C_6H_6 + C_6H_5^+ \rightarrow C_{10}H_8 + C_2H_3^+$$

$$C_{10}H_7 + C_4H_3^+ \rightarrow C_{14}H_{10}$$

$$C_6H_5 + C_4H_5^+ \rightarrow C_{10}H_8 + H_2$$

$$C_{10}H_7 + C_5H_5^+ \rightarrow C_{14}H_{10} + CH_2^+$$

These reactions represent radical–radical coupling processes that lead to ring condensation and extension, characteristic of the transformation from smaller unsaturated species to polycyclic aromatic hydrocarbons (PAHs).

3.8 Role of nanostructured catalysts in π–σ transformation

The catalytic influence of nanostructured Na-bentonite clay was found to accelerate radiation-induced structural rearrangements.[20] The π-electron cloud of aromatic compounds readily interacts with the catalyst surface, forming weak π-complexes that facilitate molecular reorientation. As structural reconfiguration progresses, π–σ transitions occur, leading to the formation of covalent σ-bonds between oil molecules and surface atoms of the catalyst.

This process can involve hydrogen transfer reactions—including hydrogenation, dehydrogenation, transalkylation, and cracking—which contribute to redistribution of hydrogen atoms and cleavage of C–C bonds. Nanoparticle interaction promotes cooperative effects, which may either stimulate or inhibit the formation of aromatic species and, in certain cases, facilitate the assembly of macromolecular aggregates.

3.9 Comparative analysis of oil maturity using EPR spectroscopy

Electron Paramagnetic Resonance (EPR) spectroscopy was employed to monitor the presence and transformation of paramagnetic centers in the crude oil samples before and after irradiation. As shown in Fig. 8 oils from platforms 8 and 10 exhibited no significant EPR spectral changes upon irradiation. The g-factor ($g \approx 2.0044$) and linewidth ($\Delta B = 5.27$ G) remained constant, indicating no appreciable concentration of paramagnetic species, such as vanadyl (VO^{2+}) or Ni-porphyrin complexes. This aligns with the classification of these oils as geochemically mature, lacking the reactive aromatic structures required for radiolytic transformation.

In contrast, the sample from platform 14 (Fig. 9) showed a measurable increase in line width ($\Delta B = 5.50$ G) and signal intensity post-irradiation, consistent with the formation of new carbon-centered radicals. The g-factor ($g = 2.0041$) remained within the typical range for organic radicals, but the observed changes confirm the structural immaturity of the sample and the presence of radiation-sensitive arenes and their derivatives.

3.10 Structural reorganization and aromatic depletion in mature crude oils under gamma irradiation

To evaluate the structural evolution of mature crude oil under gamma irradiation, the variation in arene content and bulk density of samples from platforms 8 and 10 was analyzed across a radiation dose range of 0–260 kGy. These samples are classified as geochemically mature, characterized by low aromaticity and the absence of high-molecular-weight asphaltenes.

3.10.1 Arene degradation dynamics. Fig. 10 shows a sharp decline in arene concentration with increasing gamma dose. Both samples initially contained ~38 wt% arenes, which steadily decreased to approximately 5.5 wt% (platform 10) and 5.2 wt% (platform 8) after 260 kGy exposure. The nearly linear trend across the dose range indicates a dose-dependent

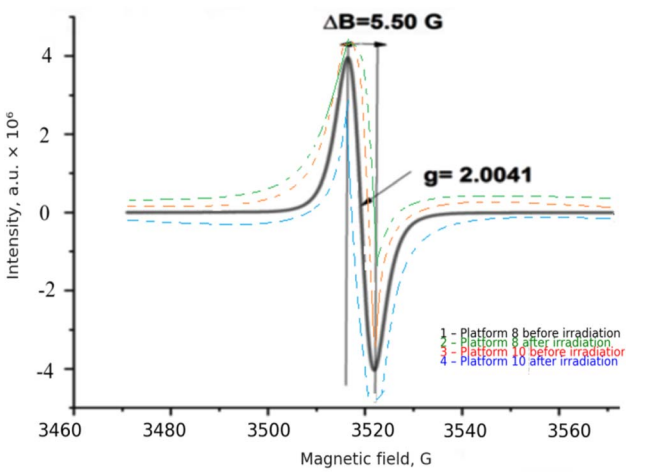

Fig. 8 EPR spectra of crude oil samples obtained from platforms 8 and 10 of the Gunashli oil field: 1 and 2 – before and after irradiation of oil from platform 8; 3 and 4 – before and after irradiation of oil from platform 10.

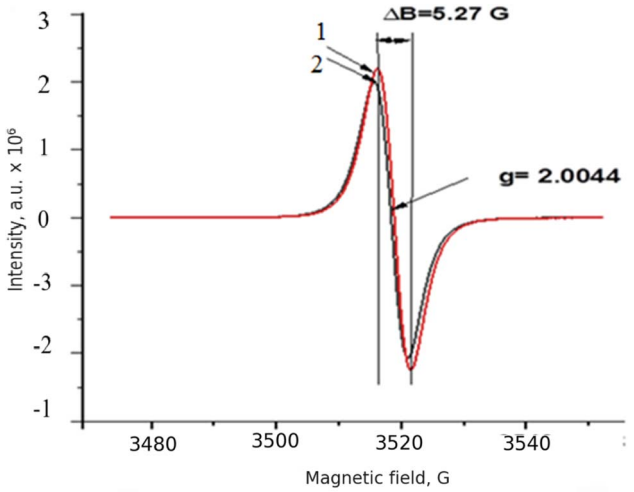

Fig. 9 EPR spectra of crude oil samples from platform 14 of the Gunashli oil field: 1 – before irradiation; 2 – after irradiation.

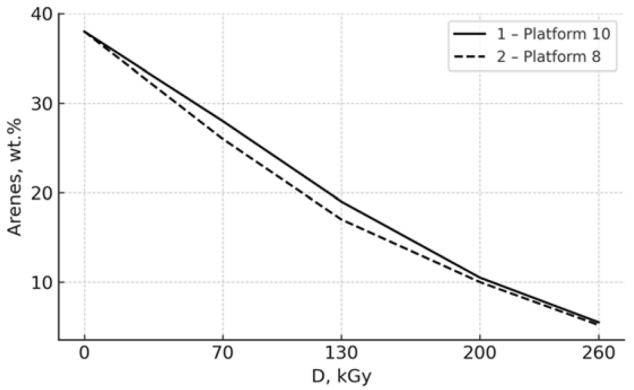

Fig. 10 Dose-dependent decrease in arene content in mature crude oil samples from platforms 8 and 10: 1 – platform 10; 2 – platform 8.

degradation mechanism. This process is attributed to the homolytic cleavage of C=C bonds in the aromatic cores, followed by hydrogen abstraction, radical recombination, and ring-opening reactions. These pathways ultimately convert π-conjugated systems into aliphatic fragments and isomeric structures with reduced resonance stabilization.

The concentration of arenes falls from 38 wt% to approximately 5.5 wt% at 260 kGy.

3.10.2 Density response and structural interpretation. Corresponding changes in density are presented in Fig. 11.

The initial density values of platform 8 and platform 10 oils were 0.864 g cm^{-3} and 0.863 g cm^{-3}, respectively. Following irradiation up to 260 kGy, these values decreased to 0.8553 g cm^{-3} (platform 8) and 0.8552 g cm^{-3} (platform 10), reflecting an approximate 1% reduction. This decrease is indicative of molecular fragmentation and the formation of lighter hydrocarbons due to the breakdown of condensed aromatic systems. The near-identical density profiles for both samples suggest compositional similarity and confirm the

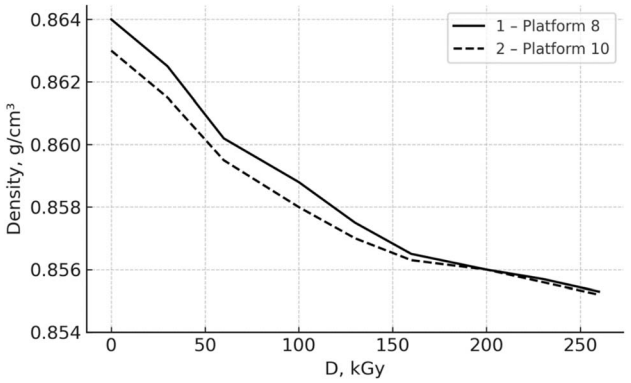

Fig. 11 Variation in density of mature crude oil samples under increasing gamma dose:1 – platform 8; 2 – platform 10. The density decreases by ~1%, indicating radiolytic fragmentation of aromatic structures.

reproducibility of the radiolytic effect across adjacent oil reservoirs.

3.10.3 Rheological implications. Although changes in molecular composition are evident, the relatively small differences in density and arene loss between the two samples imply that their rheological behavior remains largely unaffected. The oils maintain comparable viscosity and flow properties, which is consistent with their similar geological origin and molecular architecture.

3.10.4 Catalytic context. It should be noted that these experiments were conducted without the addition of catalytic agents. Nevertheless, earlier results demonstrate that nanostructured Na-bentonite clay substantially accelerates similar radiolytic transformations. The catalytic surface facilitates π–σ electron transitions and enhances the degradation of aromatic compounds through interactions with short-lived radicals. This synergy between ionizing radiation and nanostructured clays is critical for advancing radiolysis-driven oil upgrading technologies.

4 Conclusion

This study provides experimental evidence supporting the catalytic role of radiation in the metamorphism of hydrocarbons into mature petroleum, mediated by sodium-bentonite clay and gamma irradiation. The Lewis acid sites of bentonite may participate in the carbocation mechanism, but further verification is required.

The results demonstrate that gamma-induced dehydration of interlayer and pore water within nanostructured sodium-bentonite clay generates hydrogen species, which in turn promote the hydrogenation and breakdown of aromatic hydrocarbons. A progressive disappearance of arenes was observed with increasing radiation dose in mature oil samples, particularly from platforms 8 and 10 of the Gunashli field, indicating an advanced state of metamorphism. In contrast, immature oil from platform 14 retained a significant aromatic

fraction, highlighting the incomplete transformation process at lower radiation exposure.

A strong inverse correlation was identified between radiation dose and both arene concentration and sample density, suggesting that the depletion of high-molecular-weight aromatics results in lighter hydrocarbon structures. This transformation leads to a measurable decrease in oil density and confirms the effectiveness of gamma radiation in simulating geological maturation processes.

Electron Paramagnetic Resonance (EPR) spectroscopy supported these findings by confirming the absence of asphaltenes—typical of high-molecular-weight aromatic compounds—in mature samples, while their presence or partial transformation was still detectable in immature oils.

Based on the sequential molecular transformations observed (anthracene → naphthalene → benzene → cycloalkanes → alkanes), as well as EPR spectral characteristics and the radiolytic pathways involved, we conclude that Gunashli petroleum samples likely possess suggests a possible abiogenic contribution. The radiation-driven catalytic mechanism facilitated by bentonite surfaces represents a plausible synthetic route for the formation of light hydrocarbons in natural geological settings.

These findings open up potential applications in artificial maturation of immature oils and advance our understanding of nanoclay-radiation interactions in petroleum geochemistry.

Conflicts of interest

There are no conflicts to declare.

Data availability

The data that support the findings of this study are available from the corresponding author upon reasonable request. Due to the nature of the research and the format of the raw data (including spectral analyses and irradiation parameters), datasets have not been deposited in a public repository.

References

1 H. Liu, P. Yuan, Z. Qin, D. Liu, D. Tan, J. Zhu and H. He, Thermal degradation of organic matter in the interlayer clay–organic complex: A TG-FTIR study on a montmorillonite/12-aminolauric acid system, *Appl. Clay Sci.*, 2013, **80**, 398–406, DOI: **10.1016/j.clay.2013.07.005**.

2 G. C. Le, S. Bernard, A. J. Brearley and L. Remusat, Evolution of organic matter in Argueil, Murchison and Renazzo during parent body aqueous alteration: *In situ* investigation, *Geochim. Cosmochim. Acta*, 2014, **131**, 368–392, DOI: **10.1016/j.gca.2013.11.020**.

3 C. Catrinescu, C. Fernandes, P. Castilho and C. Breen, Influence of exchange cations on the catalytic conversion of limonene over Serra de Dentro (SD) and SAz-1 clays: Correlations between acidity and catalytic activity/selectivity, *Appl. Catal. Gen.*, 2006, **311**, 172–184, DOI: **10.1016/j.apcata.2006.07.029**.

4 S. Drouin, M. Boussafir, J. L. Robert, P. Alberic and A. Durand, Carboxylic acid sorption on synthetic clays in sea water: *In vitro* experiments and implications for organo-clay behaviour under marine conditions, *Org. Geochem.*, 2010, **41**(2), 192–199, DOI: **10.1016/j.orggeochem.2009.09.006**.

5 D. L. Geatches, S. J. Clark and H. C. Greenwell, Role of clay minerals in oil-forming reactions, *J. Phys. Chem. A*, 2010, **114**(10), 3569–3575, DOI: **10.1021/jp9095654**.

6 W. Johns, Clay mineral catalysis and petroleum generation, *Annu. Rev. Earth Planet. Sci.*, 1979, **7**(1), 183–198, DOI: **10.1146/annurev.ea.07.050179.001151**.

7 G. Lagaly, M. Ogawa and I. Dékány, Clay mineral–organic interactions, in *Handbook of Clay Science*, ed. Bergaya F., Theng B. K. G. and Lagaly G., Elsevier, 2006, pp. 309–377.

8 C. Pan, L. Jiang, J. Liu, S. Zhang and G. Zhu, The effects of calcite and montmorillonite on oil cracking in confined pyrolysis experiments, *Org. Geochem.*, 2010, **41**(7), 611–626, DOI: **10.1016/j.orggeochem.2010.02.002**.

9 F. D. Mango, The origin of light hydrocarbons, *Geochim. Cosmochim. Acta*, 2000, **64**(7), 1265–1277, DOI: **10.1016/S0016-7037(99)00353-3**.

10 M. K. Ismayilova, Effects of gamma-irradiation on nanostructured Na-bentonite silicate layers at room temperature, *Probl. At. Sci. Technol.*, 2021, **135**, 51, DOI: **10.46813/2021-135-051**.

11 I. I. Mustafayev, S. Z. Melikova, *et al.*, The studies on dehydration reaction mechanism of irradiated solid acid - nanostructured sodium - bentonite clay, *J. Phys. Chem. Sol.*, 2024, **25**(2), 362–367, DOI: **10.15330/pcss.25.2.362-367**.

12 M. K. Ismayilova, Influence of energy transfer in the adsorbed state of the clay at the petroleum radiolysis under gamma radiation at room temperature, *Radiat. Eff. Solids*, 2020, **175**(5–6), 472–478, DOI: **10.1080/10420150.2019.1678622**.

13 I. Mustafayev, M. K. Ismayilova and F. N. Nurmammadova, Evidence of radiocatalytic action of bentonite clay in petroleum formation: The role of dehydration reaction in hydrocarbons generation, *Sci. Collect. InterConf.*, 2022, (99), 771–776, DOI: **10.51582/interconf.19-20**.

14 H. Hasanudin, W. R. Asri, I. S. Zulaikha, C. Ayu, A. Rachmat, F. Riyanti and R. Maryana, Hydrocracking of crude palm oil to a biofuel using zirconium nitride and zirconium phosphide-modified bentonite, *RSC Adv.*, 2022, **12**(34), 21916–21925, DOI: **10.1039/d2ra03941a**.

15 M. K. Ismayilova, Review of scientific literature on the role of radiation and clay in petroleum generation, *J. Radiat. Res.*, 2017, **4**(2), 66–71.

16 M. K. Ismayilova, The changes of hydrocarbon generation under the influence of gamma radiation with bentonite, *J. Radiat. Res.*, 2019, **6**(1), 60–64.

17 M. K. Ismayilova, R. J. Qasimov, M. A. Bayramov, *et al.*, The effects of low-dose radiation on structural isomerization of Gunashli oil's hydrocarbons in presence of bentonite, *J. Radiat. Res.*, 2020, **7**(1), 57–63.

18 J. Cheng, R. Gu, P. He, *et al.*, Study on the uranium adsorption stability of high-dose γ-ray- irradiated clay,

Appl. Radiat. Isot., 2022, **181**, 110102, DOI: **10.1016/j.apradiso.2022.110102**.

19 M. K. Ismayilova, I. I. Mustafayev, S. Z. Melikova, F. N. Nurmammadova and M. H. Aliyeva, Radiation-induced isomerization reaction mechanism of hydrocarbons on the surface of solid acid, *J. Phys. Chem. Sol.*, 2023, **24**(3), 460–466, DOI: **10.15330/pcss.24.3.460-466**.

20 M. K. Ismayilova, I. I. Mustafayev, S. Z. Melikova, F. N. Nurmammadova and M. H. Aliyeva, The studies on dehydration reaction mechanism of irradiated solid acid - nanostructured sodium - bentonite clay, *J. Phys. Chem. Sol.*, 2024, **25**(2), 362–367, DOI: **10.15330/pcss.25.2.362-367**.